VIII. MICROWAVE TUBE RESEARCH

L. D. Smullin
Prof. L. J. Chu
A. G. Barrett
A. Bers
D. L. Bobroff
C. Fried
H. A. Haus
A. J. Lichtenberg
H. Shelton

A. INTRODUCTION

The principal aim of the work of this group is to achieve a better understanding of the propagation of signals and noise on long, confined electron beams. Both theoretical and experimental investigations are being carried out.

The theoretical studies are concerned with extensions of the single-velocity theory; that is, small- and large-signal klystron theory, Rack-Llewellyn noise theory applied to nonparallel flow, and multianode low-noise guns. The case of beams composed of electrons with a finite velocity spread is also being studied.

Since many of the basic physical facts about microwave signals on electron beams are poorly understood, an experimental program is being carried on in parallel with the theoretical work. One experiment is a study of noise on magnetically focused electron streams. It employs a demountable system with provision for mounting various types of electron guns, and a movable cavity for probing the noise along the electron beam. The effect of magnetic field, ion neutralization, gun design, and other parameters on the microwave noise in the beam is being studied.

A second experiment utilizes a demountable tube with two movable cavities of the klystron type. This tube is being used for a detailed study of space-charge debunching phenomena at low- and high-signal levels. It is hoped that further insight can be obtained into the transition region between small- and large-signal operation.

L. D. Smullin

B. NOISE IN ELECTRON BEAMS

The noise measurements described in the Quarterly Progress Reports of April 15, July 15, and October 15, 1953, indicated a marked difference in the results, dependent on whether the noise power measurements were performed on pulsed (almost unneutralized) or steady-current (entirely or almost neutralized) electron beams. Under pulsed conditions there was a much stronger tendency toward growing noise waves in the second half of the drift space than under steady-state operation. Also, the number and the deepness of the minima before the growing wave set in were somewhat different, depending again on whether the measurements were performed on pulsed or steady-current beams. To close the gap between these two operating conditions the following experiment was devised. Pulsing the tube with a very long (several hundred microseconds) voltage pulse would produce a beam that is unneutralized at the beginning, but reaches its final degree of neutralization toward the end of the pulse. By applying a gate of short duration to the noise output with various time delays after the leading edge of the pulse, it is possible

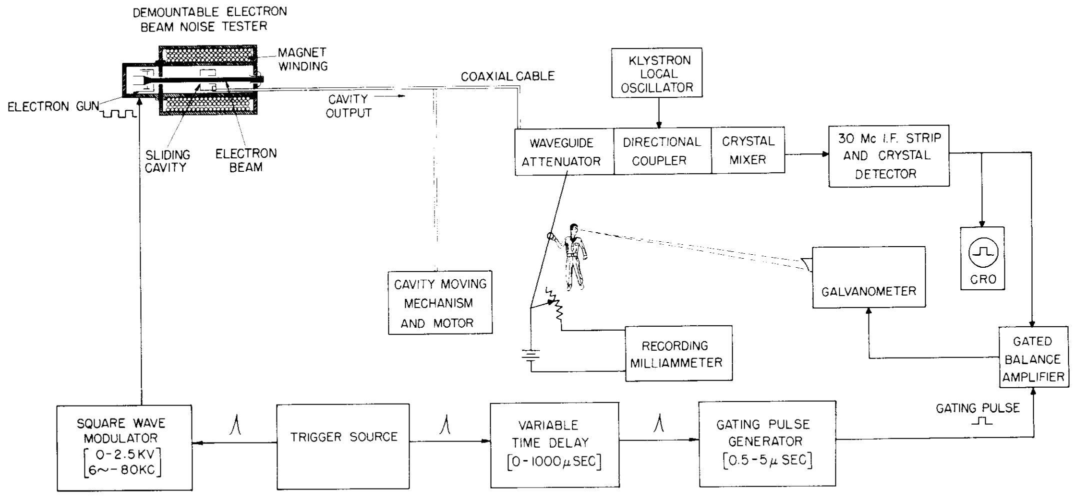

Fig. VIII-1

Block diagram of apparatus used in measuring noise at various time delays on pulsed electron beams.

to make a set of intermediate measurements between unneutralized and neutralized conditions. Figure VIII-1 shows a block diagram of the apparatus used in performing this experiment.

Our measurements were made with a convergent-flow Pierce gun with the parameters that were given in the Quarterly Progress Report of April 15, 1953. The pulse modulator maintained a 50-percent duty cycle with a variable repetition rate. First, a pulse of 500-μsec duration was applied after time delays of 4, 14, 34, 104, and 304 μsec. Thereafter the pulse length was increased to 2500 μsec, and the gating pulse was shortened to approximately 1.5 μsec. The time delays used in this case were 0, 4, 104, and 1000 μsec. The noise power curves are shown in Figs. VIII-2, VIII-3.

A comparison of these curves and the ones given in the Quarterly Progress Report of July 15, 1953, shows the transition between the unneutralized and the neutralized states. The second and the third minima in the short-pulse experiments (Quarterly Progress Report, July 15, 1953) are rather ill-defined compared to those (shown here) resulting from the long-pulse experiments with small time delay. This poor definition is probably the result of the relatively poor modulator pulse shape used during the short-pulse (0.7 μsec) measurements.

The experiments will be repeated for confined-flow electron beams.

C. Fried

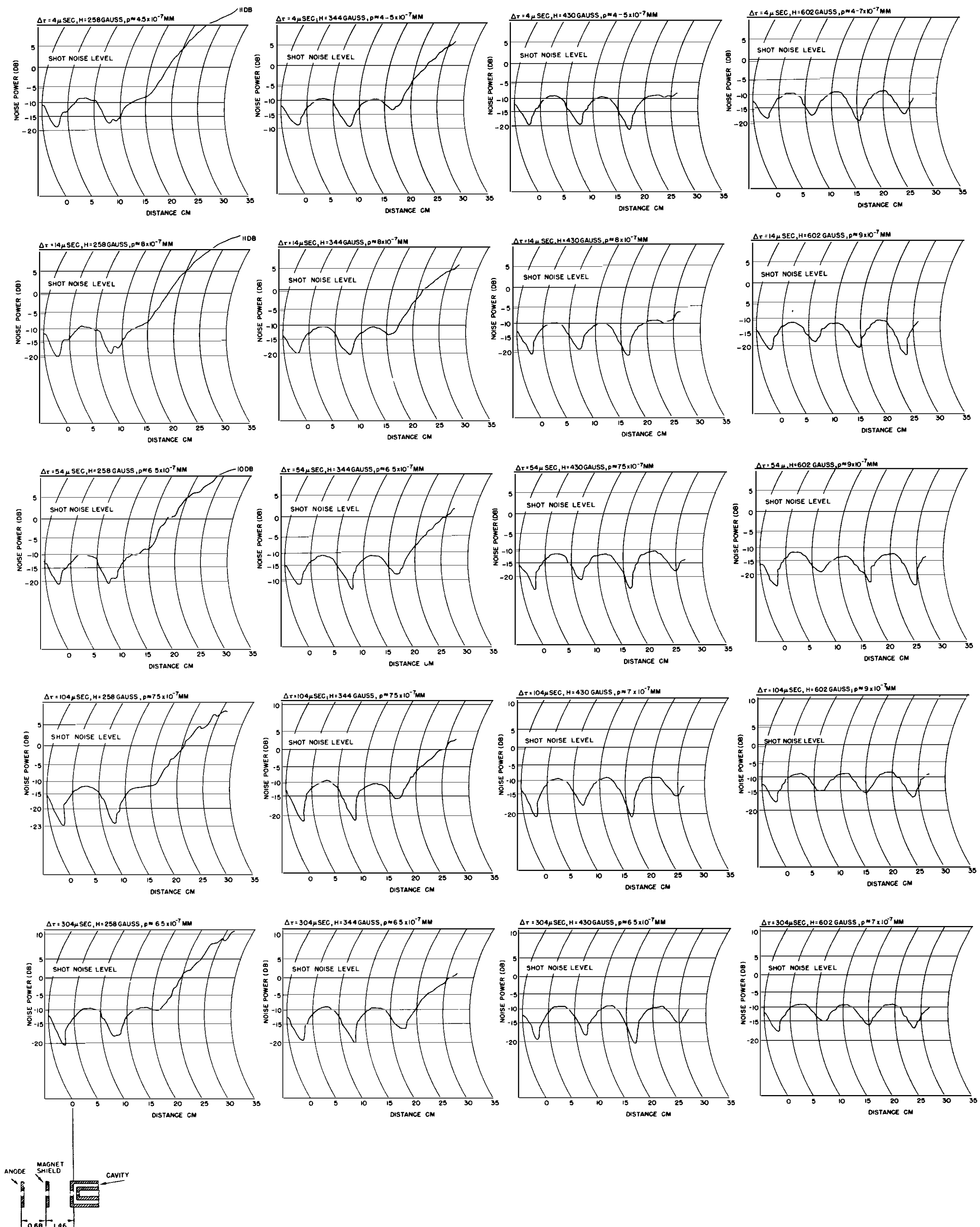

Fig. VIII-2

Noise power vs cavity position for space-charge-limited, convergent-flow, pulsed electron beam; $V_o = 1500$ volts, $I_o = 4.7$ ma, pulse duration = 500 μsec, interception current 0.1 percent, 0.1 percent, 0.2 percent, and 1.5 percent, for H = 602 gauss, 430 gauss, 344 gauss, and 258 gauss, respectively.

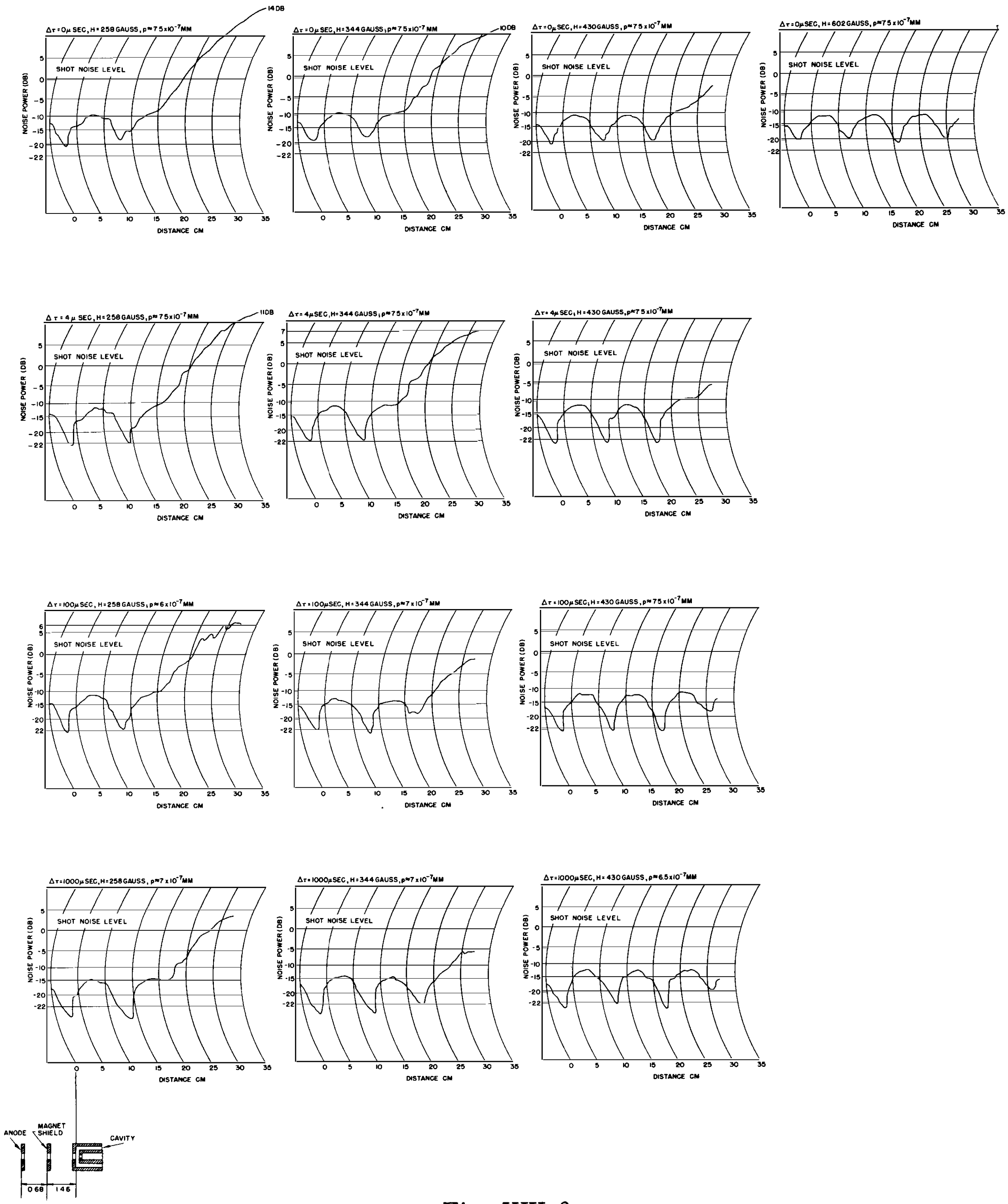

Fig. VIII-3

Noise power vs cavity position for space-charge-limited, convergent-flow, pulsed electron beam; V_o = 1500 volts, I_o = 4.7 ma, pulse duration = 2500 μsec.

C. PROPAGATION OF SIGNALS ON ELECTRON BEAMS

The large-signal measurements on a velocity-modulated electron stream reported in the Quarterly Progress Report of October 15, 1953, have been continued. The critical rf bunching voltage above which overtaking of the electrons sets in, and the maximum obtainable rf current have been experimentally determined. A comparison with a simplified theory has been made.

Re-entrant klystron cavities with grids were used in the measurements. The gap shunt resistance, R_s, of the buncher cavity was 3.2×10^5 ohms; the loaded Q, Q_ℓ, was 1340; the unloaded Q, Q_o, was 2400; and the length of the gap, d, was 0.267 cm. For the catcher cavity the values were $R_s = 1.9 \times 10^5$ ohms, $Q_\ell = 350$, $Q_o = 1100$, and $d = 0.267$ cm. Both cavities were movable along the beam. The electron gun produced a parallel beam with a diameter of 0.15 cm. The drift-tube diameter was 5 cm. Since the rf voltage across the catcher gap was small under all circumstances, the evaluation of the rf current was simplified.

The theoretical buncher-gap voltage, V_c, at which overtaking sets in, was determined from a large-signal analysis of an infinite parallel-plane electron beam. If it is assumed that no overtaking occurs in the electron beam and that the electrons move in an ion space-charge equal and opposite in sign to the space-charge of the unmodulated beam, the differential equation for the velocity of one electron is

$$\left(\frac{d^2}{dt^2} + \omega_p^2\right) v = v_o \tag{1}$$

where d^2/dt^2 is a total derivative with time, ω_p is the plasma frequency of the unmodulated beam, and v_o its velocity. With a sinusoidal velocity modulation of angular frequency, ω, (assuming a small buncher-gap voltage) the expression for the distance from the buncher gap traveled by one electron becomes

$$z = \frac{v_1}{p} \sin \omega t_o \sin \omega_p (t - t_o) + v_o (t - t_o) \tag{2}$$

where v_1 is the amplitude of the velocity modulation in the gap and t_o is the time of passage of an electron through the gap. The criterion of no overtaking, $(\partial z)/(\partial t_o) \leq 0$, gives

$$\frac{v_1}{v_o} \leq \frac{\omega_p}{\omega} \tag{3}$$

if $\omega_p/\omega << 1$. The latter inequality is satisfied in most practical cases. Equation 3 with an equality sign gives the level of modulation at which overtaking sets in. The critical gap voltage above which overtaking occurs is given by

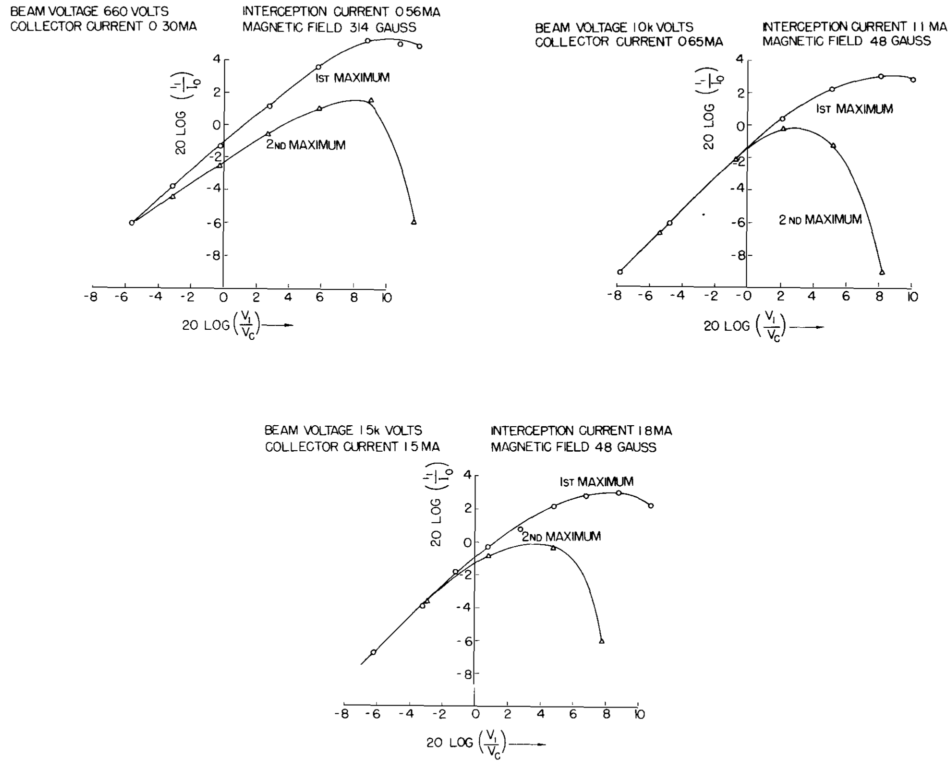

Fig. VIII-4

Plots of the magnitude of the first and second maxima of the rf beam current; V_1 is the rf voltage across the bunching gap, V_c is the theoretically computed (Eq. 4) rf gap voltage.

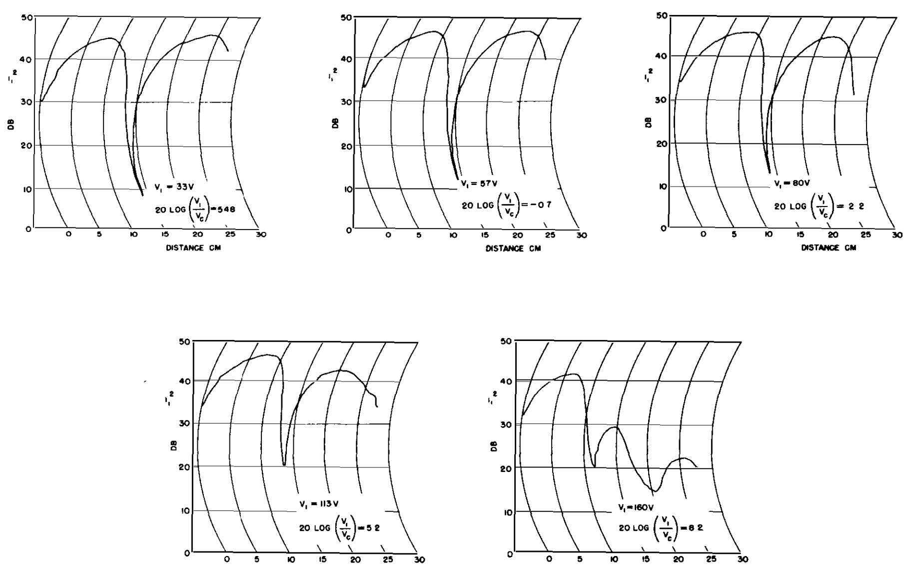

Fig. VIII-5

Standing-wave pattern of rf current; beam voltage, 1.0 kv; collector current, 0.7 ma; interception current, 1.1 ma; magnetic field, 48 gauss; M = 0.727; peak rf voltage, V_1; center of buncher gap at −1.6 cm.

$$V_c = \frac{2}{M} \frac{\omega_p}{\omega} V_o \tag{4}$$

where V_o is the voltage of the beam, and M is the beam coupling coefficient of the gap. Equation 2 can be used to find the amplitude of the fundamental harmonic of the rf current in the beam.

$$i_1 = 2 I_o J_1 \left(\frac{1}{2} M \frac{V_1}{V_o} \frac{\omega}{\omega_p} \sin \frac{\omega_p}{v_o} z \right) \tag{5}$$

for $v_1 \ll v_o$; J_1 is the first-order Bessel function.

Webster first derived the last expression by a different method. Equation 5 predicts an rf current periodic with distance.

The reduction in the axial space-charge forces resulting from the finite size of an actual beam can be taken into account by a plasma frequency reduction factor that can be determined from a small-signal analysis.

In the experiment, the rf beam current was measured as a function of distance from the buncher gap at different buncher-gap voltages, beam voltages, and magnetic focusing fields. Figure VIII-4 shows plots of the rf current at the first and second current maxima (normalized to the direct current in the beam) vs the bunching voltage. The bunching voltage is normalized to the theoretical critical voltage found from Eq. 4. The beam voltage is used as a parameter. Except at low beam voltages, the strength of the magnetic focusing field seems to have had only a small effect on the character of the curves.

At bunching voltages below the critical voltage, Eq. 5 predicts a periodic standing wave of rf beam current. Figure VIII-4 shows that the standing wave observed experimentally was periodic up to a certain critical buncher voltage. Above that voltage the second current maximum drops below the first maximum. It may be assumed that Eq. 5 is invalid above that critical input power level because overtaking has set in.

Above the critical voltage the second maximum deteriorates rapidly. The space-charge standing-wave pattern disappears. The bunching process under these conditions seems to be the result of a combined effect of electron plasma oscillations and kinematic bunching. Figure VIII-5 presents a set of curves taken at a beam voltage of 1 kv which shows the rf beam current as a function of distance at different buncher voltages. The ordinate is referred to an arbitrary level.

H. A. Haus

D. LOW-NOISE GUN DESIGN

Calculations using the Rack-Llewellyn equations indicate that an improvement of the order of 2 db in noise figure may be obtained if the region between the first and second anodes is made to produce a specified value of ζ, as compared to the performance of a region with zero current modulation at the second anode.

A gun design is being computed so that the validity of the one-dimensional analysis can be checked.

A. Bers, L. D. Smullin

E. HELIX COUPLINGS

In order to couple power into or out of a traveling-wave tube or a backward-wave oscillator, two problems must be solved: the transfer of power from a helix to a conventional transmission system; and the transfer of power from a structure in a vacuum at a high dc potential to one in air at ground potential. These problems may be solved independently or in one step.

It has been found theoretically by R. Kompfner (private communication to L. D. Smullin) and others, that power can be coupled between two oppositely wound infinite helices of equal phase velocities with a beat wavelength given by

$$\Lambda_b = \frac{\lambda}{x + b}$$

where λ is the helical wavelength, x is the normalized mutual reactance, and b is the normalized mutual susceptance. In a $(\Lambda/4)$ distance all the power from one helix would be transferred to the other. Determination of this length, either theoretically or experimentally, essentially solves the second problem, leaving the first to be solved independently.

One approach to the first problem is to match the impedance of a helix within a shield to that of a coaxial line, and then to join the two as smoothly as possible. Using the structure shown in Fig. VIII-6(a) the voltage standing-wave ratio (VSWR) of Fig. VIII-7 was obtained. Rapid fluctuations are probably due to line resonances between connector and coaxial helix connection.

After trying several helices of various pitch angles, we obtained two concentric, oppositely wound helices with a dielectric between them and having equal phase velocities within one percent. Theoretical calculation of Λ_b was made by using the approximate relationship

$$x^2 = b^2 = \frac{K_o(\beta a_2)\, I_o(\beta a_1)}{K_o(\beta a_1)\, I_o(\beta a_2)}$$

where K_o and I_o are the modified Bessel functions, β is the helix phase velocity, and a_1 and a_2 are inner and outer helix radii, respectively. Experimentally, Λ_b was determined to be 50 percent larger than the calculated value. The source of the discrepancy has not yet been discovered.

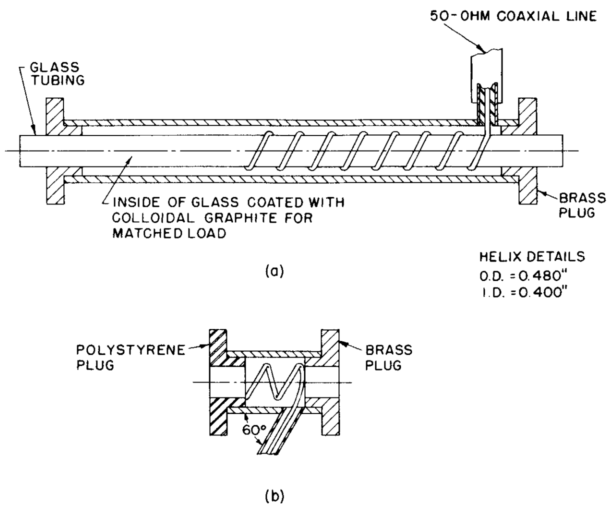

Fig. VIII-6
Test structure (a) for helix-to-helix coupling (b).

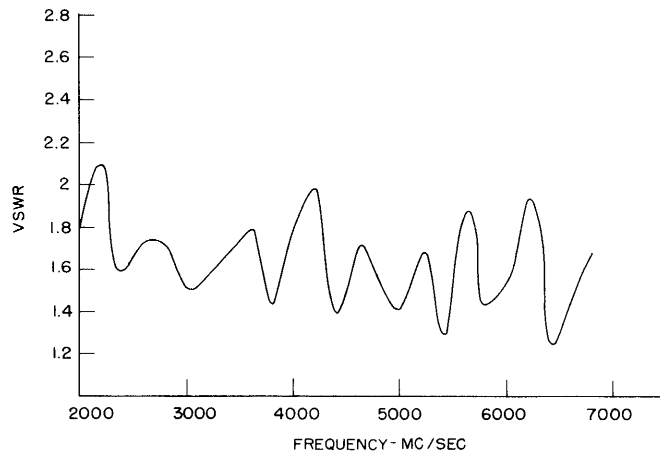

Fig. VIII-7
VSWR of test structure vs frequency.

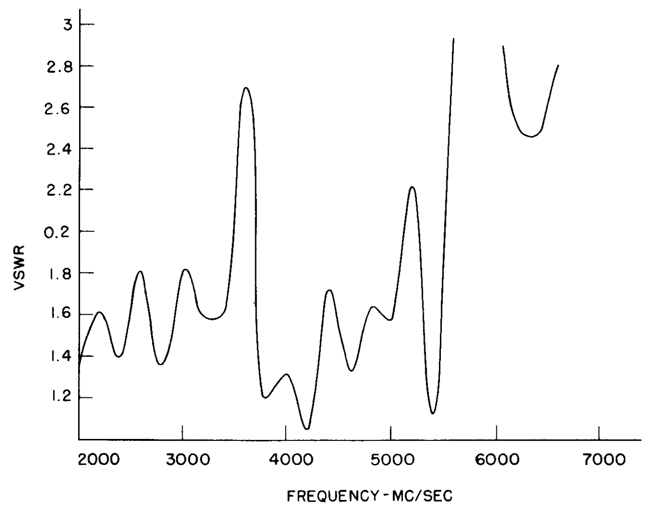

Fig. VIII-8
VSWR of helix-to-helix coupling vs frequency.

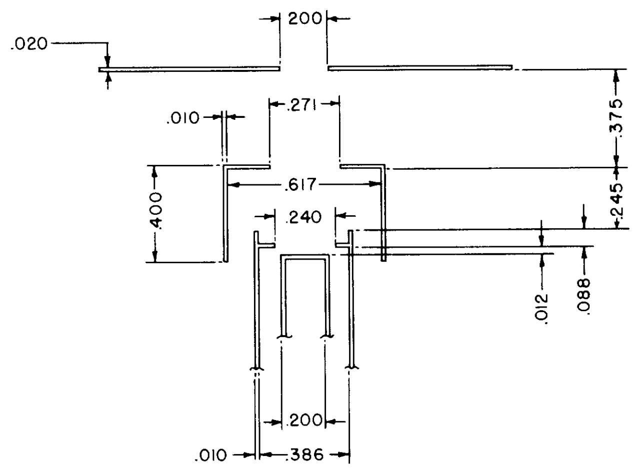

Fig. VIII-9
Essential dimensions of gun.

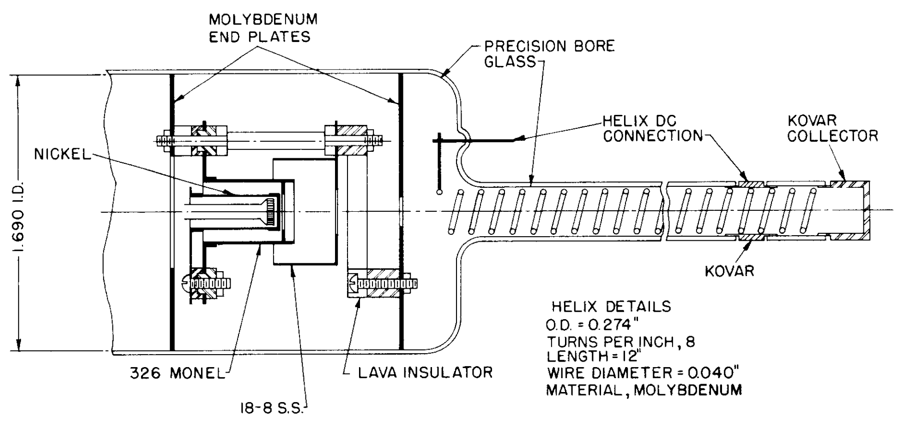

Fig. VIII-10
Backward-wave oscillator tube.

A helix-to-helix coupling, Fig. VIII-6(b), was constructed by means of the general design parameters found above. The length of the $(\Lambda_b/4)$ coupling helix was taken from the experimental value of Λ_b. The VSWR obtained is shown in Fig. VIII-8. Directivity of better than 20 to 1 was obtained from 2 kMc/sec to 4 kMc/sec.

A. J. Lichtenberg

F. BACKWARD-WAVE OSCILLATOR

Following unsuccessful attempts to obtain oscillations from the tube described in the Quarterly Progress Report of April 15, 1953, the tube was redesigned electrically and mechanically, as shown in Figs. VIII-9 and VIII-10.

Prototypes of the new tube have oscillated between 2800 Mc/sec and 6000 Mc/sec with a beam voltage variation of 500-5200 volts.

The tube showed best operation with the highest axial magnetic field – approximately 800 gauss. Although the first anode and cathode were designed to produce a parallel beam, about the size of the helix, the second anode has a focusing action that reduces the beam diameter, thus reducing the coupling to the helix. The large magnetic field tended to keep the beam at its full diameter. Collector current was greatest with the magnetic field somewhat skew to the axis of the gun. This was probably the result of internal misalignment. The largest oscillations, however, were noticed with the field oriented slightly differently. A small positive bias applied to the cathode electrode spread the beam and improved the low-frequency output considerably.

A helical coupling similar to that shown in Fig. VIII-6(b) was used. Output power varied greatly with frequency and was discontinuous for low beam currents. R. Kompfner (Proc. I. R. E. 41, 1602-1611, 1953) explained a similar variation as an inhibiting effect caused by strong modes. In our case, the pattern could be controlled by the axial position of the coupling.

A. G. Barrett, A. J. Lichtenberg